

A new approach to BOR-FDTD Subgridding

Wouter Tierens
Ghent University

Department of Information Technology
Email: wouter.tierens@intec.ugent.be

Daniël De Zutter
Ghent University

Department of Information Technology
Email: daniel.dezutter@intec.ugent.be

Kristof Cools*
Ghent University

Department of Information Technology
Email: kristof.cools@intec.ugent.be

Abstract—In this paper the approach followed by Chilton et al. to develop a provably passive and stable 3D FDTD subgridding technique, is adapted to Body-Of-Revolution (BOR) FDTD. To this end a new set of basis functions is presented together with the mechanism to assemble them into an overall mesh consisting of coarse and fine mesh cells. To preserve the explicit nature of the leapfrog time stepping algorithm, appropriate mass-lumping concepts, again specifically adapted to the BOR-FDTD situation, are invoked. Numerical examples for toroidal cavities demonstrate the stability and accuracy of the method.

I. INTRODUCTION

Amongst nowadays numerical techniques to solve Maxwell's equations, the Finite Difference Time Domain (FDTD) method [1] is one of the most powerful tools. It is massively parallelizable, matrix-free in contrast to finite-element (FE) techniques, does not require the knowledge of suitable Green's functions, as is the case for integral equation methods and can handle complex geometries. In the past decades a lot of advances have been made with respect to absorbing boundary conditions, dispersion-relation preservation, subgridding, unstructured grids etc. For a review on these advances we refer to [2], [3] and the references therein and to the huge body of literature on these topics. The research presented below is motivated by the study of complex wave phenomena in Tokamak plasmas [4], [5] such as to be used in ITER. In order to be able to predict all relevant wave phenomena in such plasmas, one must be able to correctly model transition regions where the solutions of the dispersion relation can change quite abruptly, involving the sudden and localized appearance of solutions with a wavelength many times shorter than the usual wavelength, the so-called *mode conversion* [5]. Subgridding is mandatory in order to take these crucially important, but very different length scales, into account.

Here, a brief account is given of our efforts to develop a suitable BOR-FDTD subgridding technique which can of course also be used outside the context of plasma research. For an introduction to BOR-FDTD we refer to Chapter 12 of [1] and to a.o., [6], [7]. Subgridding has been thoroughly investigated in the past e.g. in [8], [9], [10], [11].

II. BOR-FDTD DISCRETISATION

The classical BOR-FDTD representation of [1] is used as our starting point. Fig. 1 shows a unit BOR-FDTD cell with material parameters ϵ and μ centered on the B_θ component, extending from $r = R_0$ to $r = R_0 + \Delta$ and from $z = Z_0$ to

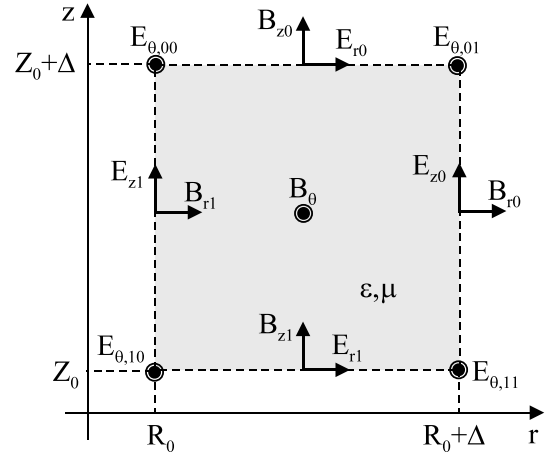


Fig. 1. A Yee-like unit cell in BOR-FDTD showing the anchor points of the basis functions.

$z = Z_0 + \Delta$. For each angular mode number M , the following 8 new basis functions \vec{E}_n for the electric field are introduced:

$$E_{ri} = \left(\begin{cases} \frac{z-Z_0}{\Delta} & i = 0 \\ 1 - \frac{z-Z_0}{\Delta} & i = 1 \end{cases} \right) \cos(M\theta) \vec{1}_r \quad (1)$$

$$E_{\theta,ij} = \left(\begin{cases} \frac{z-Z_0}{\Delta} & i = 0 \\ 1 - \frac{z-Z_0}{\Delta} & i = 1 \end{cases} \right) \cdot \left(\begin{cases} f_1(r) & j = 0 \\ f_2(r) & j = 1 \end{cases} \right) \sin(M\theta) \vec{1}_\theta \quad (2)$$

$$E_{zi} = \left(\begin{cases} \frac{r-R_0}{\Delta} & i = 0 \\ 1 - \frac{r-R_0}{\Delta} & i = 1 \end{cases} \right) \cos(M\theta) \vec{1}_z \quad (3)$$

with $f_1(r) = \frac{R_0}{\Delta} \left(\frac{R_0+\Delta}{r} - 1 \right)$ and $f_2(r) = \frac{R_0+\Delta}{\Delta} \left(1 - \frac{R_0}{r} \right)$. These basis functions are zero outside the considered cell. The corresponding basis functions \vec{B}_n for the magnetic induction are:

$$B_{ri} = \frac{(R_0 + (1-i)\Delta) \sin(M\theta)}{r} \cdot \left(\begin{cases} \frac{r-R_0}{\Delta} & i = 0 \\ 1 - \frac{r-R_0}{\Delta} & i = 1 \end{cases} \right) \vec{1}_r \quad (4)$$

$$B_\theta = \cos(M\theta) \vec{1}_\theta \quad (5)$$

$$B_{zi} = \frac{(R_0 + \Delta/2) \sin(M\theta)}{r} \cdot \left(\begin{cases} \frac{z-Z_0}{\Delta} & i = 0 \\ 1 - \frac{z-Z_0}{\Delta} & i = 1 \end{cases} \right) \vec{1}_z \quad (6)$$

Crucial to the method is that these magnetic induction basis functions have the *curl inclusion* property, i.e.

$$\forall \alpha_n \exists \beta_n : \vec{\nabla} \times \sum_n \alpha_n \vec{E}_n = \sum_n \beta_n \vec{B}_n \quad (7)$$

meaning that the curl of every electric basis function (and, by extension, of any linear combination of electric basis functions) can be written as a linear combination of magnetic basis functions.

Next, the electric field \mathbf{E} and the magnetic induction \mathbf{B} are expanded in the basis functions \vec{E}_n resp. \vec{B}_n . The expansion coefficients, which still depend on time, are collected in the column vectors \mathbf{e} and \mathbf{b} . As a consequence of the curl inclusion property, Faraday's law within a single BOR-FDTD cell can now be satisfied exactly. This is not the case for Ampere's law. This law is enforced in the *weak* sense by testing both sides of Maxwell's second curl equation with the electric field basis functions. This finally leads to the following discretised form of Maxwell's equations:

$$C\mathbf{e}(t) = -\frac{d\mathbf{b}(t)}{dt} \quad (8)$$

$$[\star_\epsilon]^{-1} C^T [\star_\mu^{-1}] \mathbf{b}(t) = \frac{d\mathbf{e}(t)}{dt} \quad (9)$$

The discrete curl matrix C depends explicitly on the mode number M and the radial cell position, as is expected from the behaviour of the continuous curl operator in cylindrical coordinates. Explicitly, C^T is given by

$$\begin{bmatrix} 0 & 0 & \frac{1}{\Delta} & \frac{M}{R_0+\Delta/2} & 0 \\ 0 & 0 & \frac{-1}{\Delta} & 0 & \frac{M}{R_0+\Delta/2} \\ 0 & \frac{-1}{\Delta} & 0 & \frac{-R_0}{\Delta(R_0+\Delta/2)} & 0 \\ \frac{-1}{\Delta} & 0 & 0 & \frac{R_0+\Delta}{\Delta(R_0+\Delta/2)} & 0 \\ 0 & \frac{1}{\Delta} & 0 & 0 & \frac{-R_0}{\Delta(R_0+\Delta/2)} \\ \frac{1}{\Delta} & 0 & 0 & 0 & \frac{R_0+\Delta}{\Delta(R_0+\Delta/2)} \\ \frac{-M}{R_0+\Delta} & 0 & \frac{-1}{\Delta} & 0 & 0 \\ 0 & \frac{-M}{R_0} & \frac{1}{\Delta} & 0 & 0 \end{bmatrix} \quad (10)$$

The curl inclusion property, together with the existence of a left inverse of the C^T matrix, implies that every magnetic induction basis function can be written as a linear combination of the curl of the electric basis functions.

$[\star_\mu^{-1}]$ and $[\star_\epsilon]$ are the mass matrices obtained by integrating scalar products of basis functions over the whole problem volume.

$$[\star_\mu^{-1}]_{n,m} = \int \mu^{-1} \vec{B}_n \cdot \vec{B}_m dV \quad (11)$$

$$[\star_\epsilon]_{n,m} = \int \epsilon \vec{E}_n \cdot \vec{E}_m dV \quad (12)$$

The integration over θ is performed analytically, yielding a factor of π . The remaining integration over r and z is done using trapezoidal integration (*mass lumping* [12]) with sampling points at the 4 cell corners. This makes these matrices diagonal and positive definite. If $O(\Delta^4)$ terms in $[\star_\mu^{-1}]$ are neglected, this method reduces exactly to classical BOR-FDTD.

III. SUBGRIDDING BASIS FUNCTIONS

Suppose that subgrids of size $\Delta/N \times \Delta/N$, with N an integer, are introduced. In order to be able to apply the theory of [13], asserting that the resulting scheme is indeed conservative and stable, the basis functions on the fine grid must be such that a linear combination of them yields the basis functions of the coarse grid (the *nesting property*). It is easy to verify that the basis functions defined above have this nesting property.

In general, we can combine disjoint cells using *restriction operators*, which map disjoint basis functions (defined on a single cell) onto joint basis functions defined in the entire simulation domain, and with appropriate continuity properties. These joint basis functions cover several cells but still remain localized. As the joint basis functions are linear combinations of disjoint ones, the restriction operators can be written in matrix form.

Let A_E be the restriction operator for the electric fields and A_B for the magnetic inductions. Using these operators, the Maxwell curl equations for the *complete* mesh become

$$C_{joint} \mathbf{e}(t) = -\frac{d\mathbf{b}(t)}{dt} \quad (13)$$

$$[\star_\epsilon]^{-1} C_{joint}^T [\star_\mu^{-1}] \mathbf{b}(t) = \frac{d\mathbf{e}(t)}{dt} \quad (14)$$

$$[\star_\epsilon] = A_E [\star_\epsilon]_{disjoint} A_E^T \quad (15)$$

$$[\star_\mu^{-1}] = A_B [\star_\mu^{-1}]_{disjoint} A_B^T \quad (16)$$

$$C_{joint} = (A_B A_B^T)^{-1} A_B C_{disjoint} A_E^T \quad (17)$$

In 2D TE problems, the joint mass matrix $[\star_\epsilon]$ remains diagonal after restriction. In BOR-FDTD, this is still true for all components except for the θ -component of the electric field which has to be restricted in both the r and the z directions. Details will be given at the oral presentation.

IV. NUMERICAL EXAMPLES

To give the reader an indication on the stability of the method, an explicit calculation of the eigenvalues of the update matrix for a very small problem (Figs. 2 and 3) shows that the eigenvalues are all on the unit circle provided that the Courant condition for the smallest cells is respected or in this case even for a slightly higher value.

As a second example, consider a perfectly conducting torus with a square cross section from $r = 2$ m to $r = 4$ m and a height of 2 m (Fig. 5), $\Delta_{coarse} = 1$ cm, $\Delta_{small} = 1/3$ cm. The fine grid is a square from $r = 2.6$ m $z = 0.6$ m with sides of 34 cm, as indicated by the rectangle. The cavity is partly filled with a dielectric material with $\epsilon = 9\epsilon_0$ at $r > 3.5$ m. The mode number $M = 5$ and the source has a Gaussian spectrum centered at $\omega_0 = 3.3$ GHz. The resulting spectrum is shown in Fig. 4, and the typical behaviour of the electric field in figure 5. The presence of the subgrid area barely disturbs the vertical symmetry of the situation and doesn't significantly change the resonance spectrum. Further examples will be provided in the oral presentation.

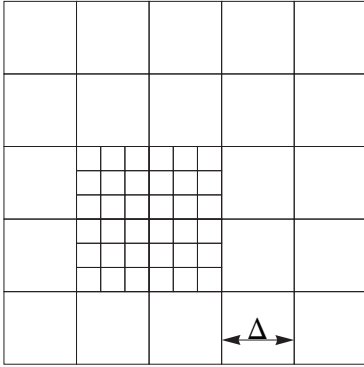


Fig. 2. A simple configuration for the exact eigenspectrum calculation.

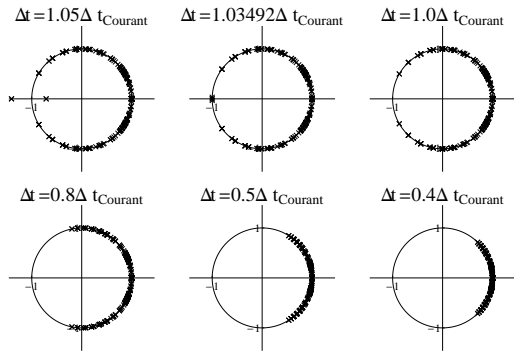


Fig. 3. The eigenspectrum of the discrete amplification matrix for the simple configuration of Fig. 2 and for various values of Δt .

V. CONCLUSION

We have extended the provably stable subgridding method of [14] to BOR-FDTD. Using appropriate mass-lumping techniques yields an explicit and stable time-stepping algorithm provided the Courant limit of the fine mesh cells is respected (although the mass-lumping can lead to a relaxing of this limit). Examples, using toroidal cavities, have demonstrated that the proposed subgridding is indeed stable.

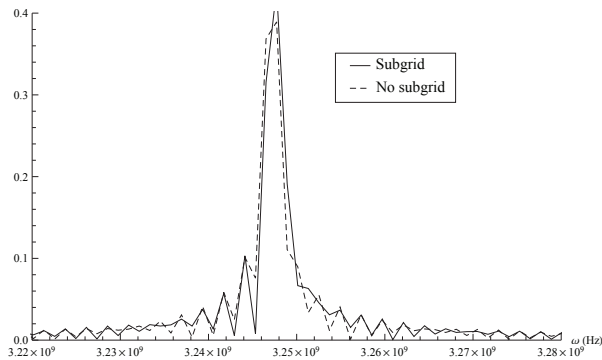


Fig. 4. Comparison between a subgridded and a non-subgridded cavity for a toroidal $M=5$ mode with a resonance frequency near 3.25 GHz

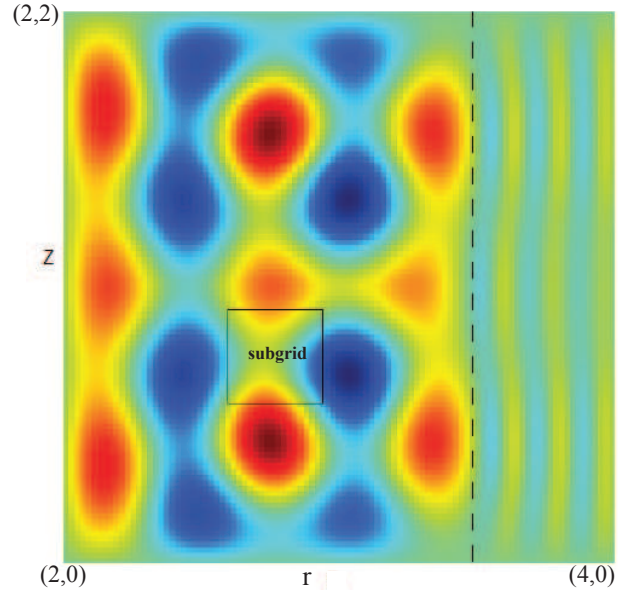


Fig. 5. $|E_\theta|$ after 10^4 steps. The rectangle indicates the boundary of the subgridded domain.

REFERENCES

- [1] A. Taflov, *Computational Electrodynamics : The Finite-Difference Time-Domain Method*. Artech House, 1995.
- [2] F. L. Teixeira, "FDTD/FETD methods: a review on some recent advances and selected applications," *Journal of Microwaves and Optoelectronics*, vol. 6, no. 1, pp. 83–95, Jun. 2007.
- [3] T. D. Tsiboukis, *Synthesis Lectures on Computational Electromagnetics*. Morgan & Claypool Publ., 2006.
- [4] D. N. Smithe, "Finite-difference time-domain simulation of fusion plasmas at radiofrequency time scales," *Physics of Plasmas*, vol. 14, no. 14, pp. 2537–2549, Apr. 2007.
- [5] T. Stix, *Waves in Plasmas*. American Institute of Physics, 1992.
- [6] J. Y. J. Shibayama, B. Murakami and H. Nakano, "LOD-BOR-FDTD algorithm for efficient analysis of circularly symmetric structures," *IEEE Microwave and Wireless Components Letters*, vol. 19, no. 2, pp. 56–58, 2009.
- [7] J. Chen and J. Wang, "A novel body-of-revolution finite-difference time-domain method with weakly conditional stability," *IEEE Microwave and Wireless Components Letters*, vol. 18, no. 6, pp. 377–379, 2008.
- [8] B. Donderici and F. L. Teixeira, "Improved FDTD subgridding algorithms via digital filtering and domain overriding," *IEEE Transactions on Antennas and Propagation*, vol. 53, no. 9, pp. 2938–2951, 2005.
- [9] L. Kulas and M. Mrozowski, "Low-reflection subgridding," *IEEE Transactions on Microwave Theory and Techniques*, vol. 53, no. 5, pp. 1587–1592, May 2005.
- [10] D. P. K. Xiao and J. Drewniak, "A three-dimensional FDTD subgridding algorithm with separated temporal and spatial interfaces and related stability analysis," *IEEE Transactions on Antennas and Propagation*, vol. 55, no. 7, pp. 1981–1990, 2007.
- [11] J. Béranger, "A Huygens subgridding for the FDTD method," *IEEE Transactions on Antennas and Propagation*, vol. 54, no. 12, pp. 3797–3804, 2006.
- [12] R. Lee, "A note on mass lumping in the finite element time domain method," *IEEE Transactions on Antennas and Propagation*, vol. 54, no. 2, pp. 760–760, 2006.
- [13] R. A. Chilton and R. Lee, "Conservative and provably stable FDTD subgridding," *IEEE Transactions on Antennas and Propagation*, vol. 55, no. 9, pp. 2537–2549, Sep 2007.
- [14] R. A. Chilton, "H-, P- and T-refinement strategies for the finite-difference-time-domain (FDTD) method developed via finite-element (FE) principles," Ph.D. dissertation, Ohio State University, 2008.